AIAA Aviation Forum and ASCEND co-located Conference Proceedings
29 July - 2 August 2024, Las Vegas, Nevada
AIAA AVIATION FORUM AND ASCEND 2024
10.2514/6.2024-4427

Design of a Six-Tiltrotor Concept Vehicle for Urban Air Mobility

Taemin Jeong[1]
Department of Aerospace Engineering, Seoul National University, Seoul, 08826, Republic of Korea

Michael Radotich[2], Wayne Johnson[3], Christopher Silva[4]
NASA Ames Research Center, Moffett Field, CA 94035

NASA has developed a series of aircraft concepts known as reference vehicles for urban air mobility operations to facilitate research and development, enabling system-level comparisons between design candidates. In this study, new six-tiltrotor reference vehicles with full-electric and turboelectric propulsion systems were developed using the NASA Design and Analysis of Rotorcraft (NDARC) tool. The sizing results and performance metrics of these new vehicles are presented, along with comparisons to existing reference vehicles. The turboelectric six-tiltrotor is shown to be the fastest among the turboelectric reference vehicles. Although the full-electric six-tiltrotor is not as fast as the turboelectric version, it still offers considerable speed along with increased safety compared to the tiltrotor reference vehicle.

I. Nomenclature

AAM	=	Advanced Air Mobility
CAMRADII	=	Comprehensive Analytical Model of Rotorcraft Aerodynamics and Dynamics II
DGW	=	Design Gross Weight
D	=	Drag
D_{climb}	=	Horizontal distance covered in the climb segment
eVTOL	=	Electric Vertical Takeoff and Landing
ESC	=	Electronic Speed Control
HECTR	=	High Efficiency Civil Tilt Rotor
ISA	=	International Standard Atmosphere
fpm	=	Feet per minute
MSL	=	Mean Sea Level
NDARC	=	NASA Design and Analysis of Rotorcraft
P_{climb}	=	Power required in the climb segment
P_{cruise}	=	Power required in the cruise segment
q	=	Dynamic pressure
ROC	=	Rate of Climb
RPM	=	Revolutions Per Minute
TMS	=	Thermal Management System
t_{climb}	=	Time in the cruise climb segment
t_{cruise}	=	Time in the cruise segment
UAM	=	Urban Air Mobility
V_{br}	=	Best range speed
V_{max}	=	Maximum speed

[1] Graduate Student, Department of Aerospace Engineering, Seoul National University, Member AIAA
[2] Aerospace Engineer, NASA Ames Research Center
[3] Aerospace Engineer, NASA Ames Research Center, AIAA Fellow
[4] Aerospace Engineer, NASA Ames Research Center, Member AIAA

II. Introduction

Over a thousand eVTOL (Electric Vertical Take-Off and Landing) designs have been proposed over the past decade following the introduction of Urban Air Mobility (UAM) [1]. To foster research and development, NASA has published several reference vehicles that can be compared at the system level [2-9]. The configurations developed as reference vehicles include quadrotor, lift+cruise, side-by-side, quiet single main rotor, coaxial quadrotor, tiltduct, tiltwing, tiltrotor, and multi-tiltrotor (Fig. 1). Some designs feature propulsion systems or control strategy variants, providing a comprehensive overview of available design choices from both heritage design philosophies and future expectations.

Fig. 1 NASA Urban Air Mobility (UAM) reference vehicles [2-9]

This paper aims to develop a new reference vehicle called the 'six-tiltrotor' using the NASA Design and Analysis of Rotorcraft (NDARC) [10] tool. It differs from the multi-tiltrotor reference vehicle [8], which employs four tilting rotors and two fixed rotors, and the tiltrotor reference vehicle [7], which utilizes two large tilting rotors. The six-tiltrotor design incorporates six tilting rotors that provide vertical thrust in thrust-borne flight and are fully tilted in wing-borne flight.

Compared to the multi-tiltrotor, the six-tiltrotor eliminates propulsion systems or rotors that operate exclusively in one flight mode, eliminating dead weight or stopped-rotor drag in either mode of flight. In contrast to conventional tiltrotors, multiple propulsors using distributed electric propulsion enhance redundancy, potentially increasing the vehicle's resilience to failure modes.

Therefore, the six-tiltrotor reference vehicle is expected to address shortcomings of previous reference vehicles and offer valuable insights for UAM design. Figure 2 depicts a representative sketch of the six-tiltrotor design, with additional drawings provided in the Appendix.

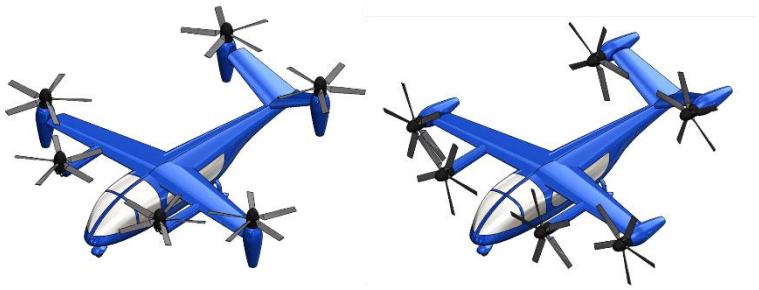

Fig. 2 Representation of six-tiltrotor concept vehicle

In the following sections, four different design variants for the six-tiltrotor reference vehicle will be presented. The propulsion system architectures chosen were full-electric (using only batteries) and turboelectric, as six rotors are not suitable for mechanical connection. Collective control and RPM control methods were compared.

The turboelectric variants were found to be lighter and faster than the full-electric variants. However, the environmental implications of UAM should be carefully considered. RPM-controlled variants resulted in heavier gross weights compared to their collective-controlled counterparts due to an additional sizing condition.

III. Six-Tiltrotor Reference Vehicle Design

Developing a new model using NDARC typically builds upon existing aircraft rather than starting from scratch. NASA reference vehicles often share identical components to maintain consistency across the vehicle group and ensure fair comparisons. For the six-tiltrotor reference vehicle, the electric tiltrotor reference vehicle [7] served as the starting point, being the most recent tiltrotor designed for the NASA UAM mission. Thus, components such as Aircraft, Systems, Cost, Emission, Landing Gear, and Fuselage were adapted from the electric tiltrotor reference vehicle. Similarly, for the turboelectric variants, models of the turboshaft engine, generator, and jet fuel tank were taken from the turboelectric lift+cruise reference vehicle.

Several design decisions were made and applied to the six-tiltrotor reference vehicle to account for its unique characteristics, and some of them were referenced from NASA's High Efficiency Civil Tilt Rotor (HECTR) [11] or the lift+cruise reference vehicle [3]. Each design decision is described in the following sections.

A. Geometry

The vehicle geometry consists of five main components: rotors, front wing, rear wing (or V-tail), fuselage, and landing gear. Among the six rotors, two forefront rotors are mounted on rotor supports connected to the inboard part of the front wing. Two rotors are mounted on the nacelle at the tip of the front wing, positioned near the middle from nose to tail. The remaining two rotors are mounted on the nacelle at the tip of the rear wing.

As speed increases from hover to cruise, the four rotors at the tips of the front wing and rear wing tilt with the nacelle, shifting the rotor positions toward the nose. The two forefront rotors at the inboard part of the front wing use a linkage mechanism to move the rotor position slightly backward while tilting. The lateral positions of the forefront rotors are fixed at the fuselage clearance value from the electric tiltrotor reference vehicle to prevent any physical interference with the fuselage.

B. Propulsion System

Two different propulsion systems are employed in the six-tiltrotor reference vehicle: full-electric and turboelectric. Both systems utilize distributed electric propulsion, where multiple electric motors individually power the rotors. Figure 3 depicts the propulsion system topology of the six-tiltrotor NDARC model, highlighting each component with specific shapes and colors. Yellow circles denote the rotors, arranged to illustrate their relative positioning on the aircraft from a top view (not to scale). Orange arrows surrounding the rotors indicate their rotational directions.

Each rotor connects to a two-stage gearbox (orange trapezoid), which then links to an electric motor (blue circle). The gearbox allows for varying tip speeds during hover (550 ft/s, consistent with other NASA reference vehicles) and cruise (with a 50% reduction). Both collective-controlled and RPM-controlled designs incorporate these two-stage gearboxes.

In the turboelectric model, additional components are integrated: a fuel tank containing jet-A fuel (green square), connected to a turboshaft engine (green circle). The turboshaft engine drives a generator, which converts mechanical power to electric power.

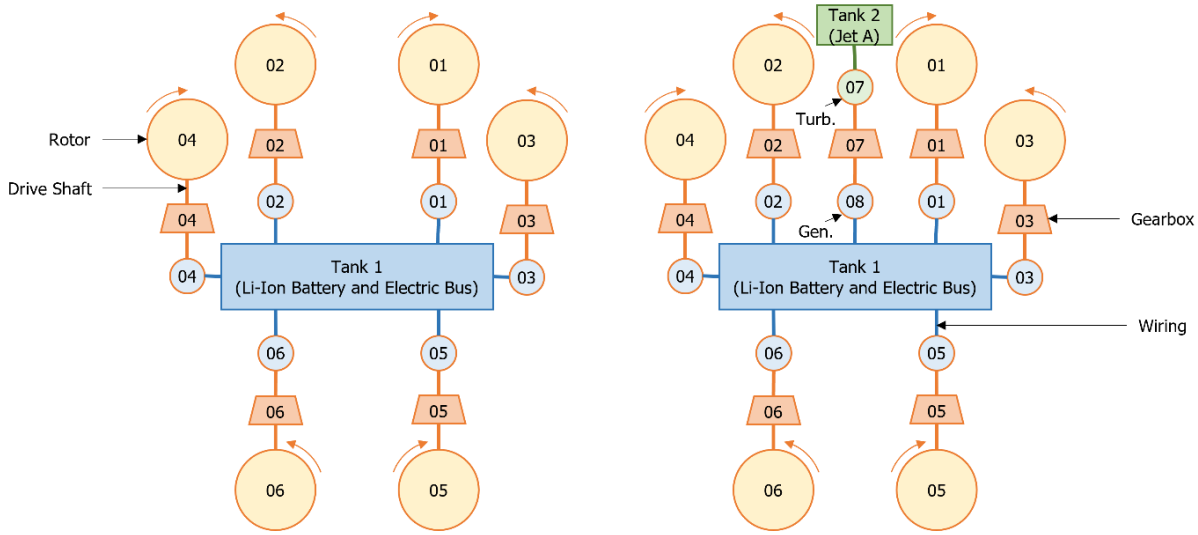

Fig. 3 Representation of full-electric (left) and turboelectric (right) power topologies

C. Control Scheme

As a tiltrotor, the six-tiltrotor vehicle used two different control schemes for helicopter mode and airplane mode. Helicopter mode includes taxi, vertical takeoff, vertical landing, and hover, whereas airplane mode refers to cruise climb, level cruise, and cruise descent. Unlike conventional rotorcrafts, the differential thrust of rotors was used for longitudinal and lateral attitude control in helicopter mode rather than cyclic pitch. Therefore, rotors were assumed to be compact and rigid without cyclic control capability.

In airplane mode, control surfaces of the front and rear wings were used for attitude control, while rotor collective pitch was adjusted for forward speed. Differential thrust could be generated in two ways: by changing collective pitch or RPM among rotors. Both collective-controlled and RPM-controlled six-tiltrotor vehicles were designed. For RPM-controlled variants, an additional control variable for blade pitch angle was implemented to achieve the blade pitch necessary for 550 ft/s hovering RPM.

For the turboelectric variants, generator current was added as a control parameter, following the approach used in the turboelectric lift+cruise reference vehicle [3].

D. Rotor

NDARC uses rotor performance parameters to calculate aerodynamic forces and power across various operating conditions. For the six-tiltrotor model, initial blade geometry and rotor performance parameters were based on those of the electric tiltrotor reference vehicle. Future studies will update this rotor model by calibrating the parameters using CAMRAD-II [12], followed by design iterations with NDARC.

Both HECTR and the tiltrotor reference vehicles model drag from the rotor and nacelle as a single component: spinner drag. The tiltrotor reference vehicle used the same fixed D/q value for the spinner as HECTR, but it was not suitable for the much smaller rotors of the six-tiltrotor reference vehicle. Therefore, spinner drag was calculated using fraction inputs from HECTR, which scales wetted area with rotor radius.

Unlike the tiltrotor reference vehicle, the six-tiltrotor reference vehicle requires two supporting arms that connect the front wing and the forefront rotors. Therefore, the weight and drag from the rotor supports were modeled by scaling from the lift+cruise reference vehicle according to their respective lengths. The rotor support length of the lift+cruise reference vehicle was defined as half of the boom length. For the six-tiltrotor reference vehicle, the rotor support length was defined as the center-to-center length of the front and mid rotors, invariant to the rotor loading or wing loading. Drag coefficients were also retrieved from the lift+cruise reference vehicle.

E. Wing

While the aerodynamic model of the wing remained the same as that of the electric tiltrotor reference vehicle, the geometry was modified. The front wing was modeled with three panels. Two mid-position rotors are mounted on the edge of the last panel. The first panel and the other two panels have different dihedral angles. The last panel near the tip has a flaperon, which can decrease download from the rotor at a slow speed. V-tail (referred to as the rear wing throughout the paper) was modeled as a wing with a large dihedral and forward sweep angle value to implement tiltrotor wing weight equations. Its control surfaces operate as a ruddervator, which controls the pitch and yaw angle of the vehicle.

The natural frequencies at which the wing vibrates are crucial in determining the wing's stiffness and weight. For instance, HECTR and the tiltrotor reference vehicle used higher frequency values because a tiltrotor with large and heavy rotors and engines needed a stiffer wing to mitigate whirl-flutter. In contrast, other reference vehicles with multiple small rotors and motors on the wing (such as multi-tiltrotor and tiltwing) used lower frequency values because the distributed propulsors on the main wing allowed the required wing stiffness to be reduced. Therefore, the same criteria were applied to the six-tiltrotor reference vehicle. Further improvement should be made regarding the wing model with multiple rotors considering whirl-flutter requirements by structural analysis.

F. Motor Model

The motor model for electric motors was retrieved from the electric tiltrotor reference vehicle with a slight change. Motor weight was modeled based on the required torque, prompting RPM-controlled variants to use a gearbox instead of direct drive due to the substantial torque increase at lower motor speeds and corresponding weight increases. The thermal management system (TMS) was modeled additionally, with its weight and power requirements based on the design heat rejection of the battery power capacity. The electronic speed control (ESC) weight was also modeled, which is scaled from the maximum power of the motor.

G. Battery

The battery model mainly remained unchanged from the electric tiltrotor reference vehicle, which has a 650 Wh/kg cell-level specific energy, reflecting anticipated advanced technology. A thermal management system weight was additionally modeled similarly to the motor model.

Some reference vehicles modeled accessory power loss in the propulsion system (side-by-side: 5 hp, side-by-side 6 pax: 20 hp, HECTR: 150 hp, tiltrotor: 50 hp, others: 0 hp). In this study, a 20 hp battery power loss was modeled with zero accessory power loss, directly modeling battery power loss rather than transmission losses from driveshafts.

H. Sizing mission and conditions

NASA's UAM reference vehicles share the same sizing mission to ensure fair comparisons of vehicle size and performance. This mission includes two 37.5 nautical mile trips and a 20-minute cruise reserve, carrying a 1,200 lb payload. Before and after the cruise segments, which involve cruise climb and level flight under a 10-knot headwind at the best range speeds, the vehicles perform taxiing, vertical flight, transition, and hovering. The sizing mission profile is illustrated in Table 1 and Fig. 4, with the development process detailed in [13]. Additionally, the mission includes a size condition of a 500 feet per minute cruise climb at 10,000 ft altitude at the best range speed. For RPM-controlled variants, a new sizing condition was applied: hover capability at 50% maximum power at 6,050 ft, inspired by Malpica et al.'s study [14], which indicated that having an additional power margin improves the handling quality of RPM-controlled concept vehicles.

Table 1 Sizing mission segments [3]

Segment	1,10	2,11	3,12	4,13	5,14	6,15	7,16	8,17	9,18	19
Initial Alt. (MSL ISA)	6,000	6,000	6,050	6,050	6,500	6,050	6,050	6,050	6,000	10,000
Final Alt. (MSL ISA)	6,000	6,050	6,050	10,000	6,500	6,050	6,050	6,000	6,000	10,000
Time (sec)	15	30	10	t_{climb}	t_{cruise}	10	30	30	15	1200
Distance (nmi)	-	0	0	D_{climb}	37.5-D_{climb}	0	0	0	0	-
Speed	-	-	0	V_{br}	V_{br}	0	0	-	-	V_{br}
ROC (ft/min)	-	100	0	≥ 900	0	0	0	-100	-	0
Percent of Max Power	10%	100%	100%	P_{climb}	P_{cruise}	100%	100%	100%	10%	P_{cruise}

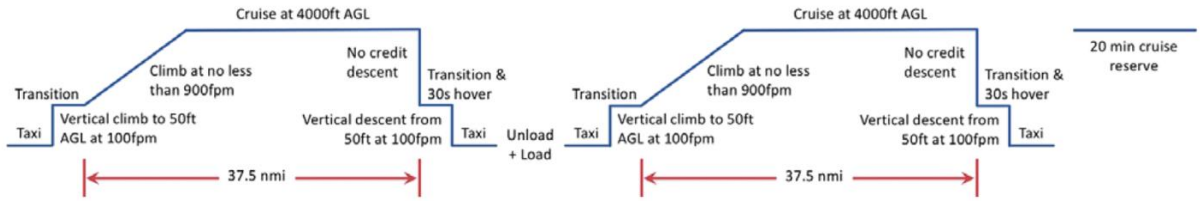

Fig. 4 NASA reference vehicle sizing mission profile [3]

IV. Design Selection

Design variables for the optimization of the full-electric and turboelectric models using collective control were defined as rotor disk loading and wing loading of the front wing. The objective was to maximize the best range speed (at DGW 6k ISA) and minimize the design gross weight, as the primary advantage of tiltrotor vehicles over other configurations using edgewise flight is faster travel time. Optimum designs were chosen from the parameter sweep, where the rotor disk loading was varied from 8 to 22 with increments of 2, and the wing loading was varied from 20 to 90 with increments of 10. Sizing results are shown in Fig. 5 and Fig. 6 for full-electric and turboelectric models, respectively. Design points were omitted if the disk loading and wing loading combination was unable to size the aircraft. Each line indicates design points with the same disk loading but different wing loading. Wing loading increases following the direction of the arrow on each line. The Pareto front, which is the line that connects non-dominated design candidates, is shown as a thick red solid line, and design candidates that construct the Pareto front are labeled.

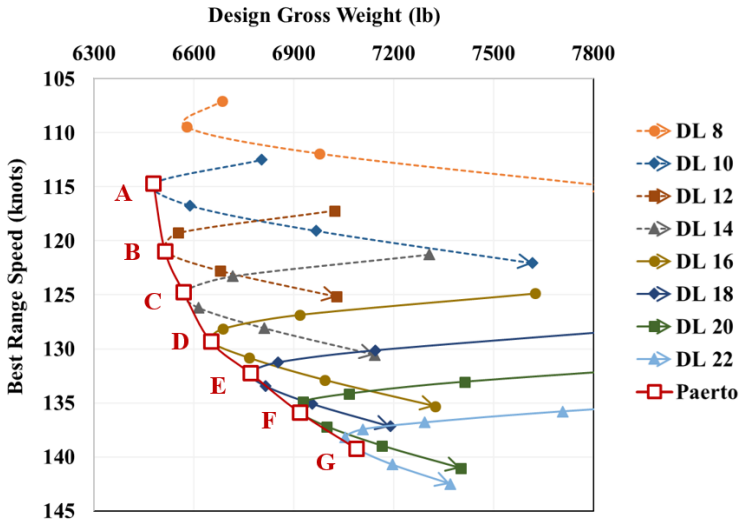

Fig. 5 Disk loading and front wing loading sweep – Full-electric, collective control

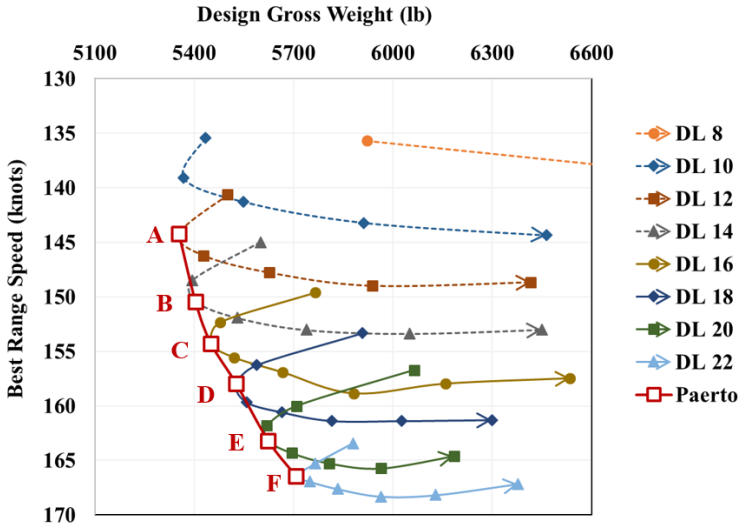

Fig. 6 Disk loading and front wing loading sweep – Turboelectric, collective control

Similar patterns were observed in both full-electric and turboelectric design sweeps. For a fixed disk loading, design gross weights decrease until a specific value of wing loading, then increase again, while the best range speed continuously increases with higher wing loading. Consequently, designs with fixed disk loading form nearly parabolic curves with a minimum design gross weight. As disk loading increases, these parabolic curves shift lower-right in Fig. 5 and Fig. 6, indicating heavier weight but faster speed.

The Pareto front, comprising non-dominated optimal design solutions (A-G for full-electric, A-F for turboelectric), was obtained. These solutions represent the most viable design options balancing best range speed and design gross weight trade-offs. To select a design from these solutions, trip operating cost, design gross weight, best range speed, and block time were compared, as shown in Table 2 and Table 3.

Table 2 Non-dominated solutions – Full-electric, collective control

Design (DL, WL)	Trip Operating Cost ($)	Design Gross Weight (lb)	V_{br} at DGW 6K ISA (kt)	Block Time (min)
A (10, 30)	588.5 (+2.4%)	6458.2 (-0.5%)	114.7 (-5.2%)	43.3 (-3.4%)
B (datum) (12, 40)	574.5	6493.2	120.9	41.0
C (14, 40)	579.4 (+0.9%)	6550.3 (+0.9%)	124.7 (+3.1%)	39.8 (+1.4%)
D (16, 50)	**579.2 (+0.8%)**	**6636.0 (+2.2%)**	**129.3 (+6.9%)**	**38.6 (+3.6%)**
E (18, 60)	585.1 (+1.9%)	6791.3 (+4.6%)	133.4 (+10.3%)	37.4 (+7.3%)
F (20, 60)	594.8 (+3.5%)	6888.4 (+6.1%)	135.8 (+12.3%)	36.8 (+9.7%)
G (22, 70)	604.1 (+5.2%)	7055.9 (+8.7%)	139.2 (+15.1%)	36.0 (+13.4%)

Table 3 Non-dominated solutions – Turboelectric, collective control

Design (DL, WL)	Trip Operating Cost ($)	Design Gross Weight (lb)	V_{br} at DGW 6K ISA (kt)	Block Time (min)
A (datum) (12, 30)	783.1	5354.1	144.2	35.9
B (14, 40)	781.4 (-0.2%)	5404.1 (+0.9%)	150.4 (+4.3%)	34.4 (-1.5%)
C (16, 40)	**795.2 (+1.5%)**	**5450.4 (+1.8%)**	**154.3 (+7.0%)**	**33.6 (-2.2%)**
D (18, 40)	812.4 (+3.7%)	5526.7 (+3.2%)	158.0 (+9.6%)	32.9 (-2.9%)
E (20, 50)	827.4 (+5.7%)	5622.9 (+5.0%)	163.2 (+13.2%)	32.3 (-3.5%)
F (22, 50)	845.4 (+8.0%)	5706.6 (+6.6%)	166.5 (15.5%)	31.8 (-4.1%)

A detailed analysis of Tables 2 and 3 revealed that the design gross weight increased at a much faster rate than the best range speed. The block time, which represented mission duration, showed a similar trend with the best range speed. Trip operating costs, however, did not follow a clear pattern due to the contrasting effects of mission time and weight. Despite this, it was evident that costs eventually increased at higher disk loadings, primarily due to weight increments. Considering the speed benefits with relatively minor losses in terms of cost and weight, designs D and C were chosen as the optimum designs for full-electric and turboelectric configurations, respectively.

For RPM-controlled variants, manipulation of blade collective pitch or initial speed was necessary in specific flight segments such as cruise climb or cruise, for each combination of disk loading and wing loading. Consequently, a design sweep was not conducted for RPM-controlled variants. Instead, RPM-controlled variants were derived for each propulsion system using the same disk loading and wing loading combinations as the selected design points for collective-controlled models with corresponding propulsion systems, even though these combinations may not be optimal for RPM control. Trip operating cost, design gross weight, best range speed, and block time for RPM-controlled variants are shown in Table 4 alongside their collective-controlled counterparts. Percent increases or decreases from collective to RPM control are provided for comparison.

Table 4 RPM-controlled counterparts

Design (DL, WL)	Trip Operating Cost ($)	Design Gross Weight (lb)	V_{br} at DGW 6K ISA (kt)	Block Time (min)
Full-electric, Coll (16, 50)	579.2	6636.0	129.3	38.6
Full-electric, RPM (16, 50)	830.3 (+43.4%)	7937.1 (+19.6%)	130.4 (+0.8%)	37.7 (-2.2%)
Turboelectric, Coll (16, 40)	795.2	5450.4	154.3	33.6
Turboelectric, RPM (16, 40)	1173.9 (+47.6%)	7175.7 (+31.7%)	164.4 (+6.5%)	32.0 (-4.9%)

RPM-controlled variants were found to be heavier than their collective-controlled counterparts in both full-electric and turboelectric designs. This weight differences were due to the additional sizing requirement to hover under a 50% power margin for RPM-controlled variants, necessitating larger electric motors. The weight and speed increases were more pronounced in the turboelectric variant, with a weight increase of over 30% and a 6.5% increase in best range speed, compared to approximately 20% weight increase and 1% speed increase for the full-electric design. Trip operating costs surged by more than 40% in both cases, primarily due to the increased weight.

Considering the marginal speed advantages relative to the cost and weight increases, collective-controlled designs were selected as the initial designs for the six-tiltrotor reference vehicle. However, RPM-controlled variants may have different optimal design points, warranting further investigation in future work.

V. Results

A. Dimensions

The resulting full-electric and turboelectric vehicle dimensions are shown in Table 5.

Table 5 Vehicle dimensions

UAM Vehicle	Turboelectric	Full-Electric	UAM Vehicle	Turboelectric	Full-Electric
Rotor			Rear Wing		
Disk Loading (psf)	16	16	Wing Loading (psf)	10	10
Number of Blades	5	5	Wingspan (ft)	10.6	11.7
Radius (ft)	4.25	4.69	Chord (ft)	3.1	3.4
Chord (ft, T weighted)	0.67	0.61	Wing Area (sq. ft)	32.7	39.8
Solidity (T weighted)	0.2284	0.2284	Taper Ratio	0.57	0.57
Taper Ratio	0.35	0.35	Aspect Ratio	3.45	3.45
Aspect Ratio	5.56	5.56	Thickness	0.23	0.23
Lock Number	5.17	5.42	Sweep (degrees)	-21.7	-21.7
Front Wing			Dihedral (degrees)	37.0	37.0
Wing Loading (psf)	40	50	Engine		
Wingspan (ft)	29.8	32.8	MRP per Motor (hp)	138.0	167.4
Chord (ft)	4.3	3.8	Turboshaft Engine sfc (lb/hp-hr, SLS MCP)	0.48	-
Wing Area (sq. ft)	128.1	124.8			
Aspect Ratio	6.9	8.6	Battery Capacity (MJ)	29	1048
Thickness	0.2	0.2	Fuel Tank Capacity (lb)	205.7	-
Sweep (degrees)	-4.4	-4.4	Battery Weight (lb)	48.4	1608.8
Dihedral (degrees)	1.27	1.27	Total Engine Weight (lb)	615.4	312.6

B. **Weight**

In Table 6, a partial weight comparison between the turboelectric and full-electric designs is shown, highlighting the percentage changes from turboelectric to full-electric. The gross weight of the full-electric design increased by 22%, primarily due to the added battery weight. Despite the turboelectric variant having a 48% heavier engine system due to the additional turboshaft engine and generator, the battery required for the full-electric design was significantly heavier. Consequently, the weights of other components such as the structure, systems, and equipment also increased for the full-electric design, except for the engine section and nacelle weights.

Table 6 Partial weight statement

Component	Turboelectric (lb)	Full-Electric (lb)	Percent Change
DESIGN GROSS WEIGHT	5450.4	6636.0	22%
WEIGHT EMPTY	4033.2	5424.0	34%
STRUCTURE	1555.9	1731.4	11%
wing group	327.9	444.0	35%
rotor group	255.5	300.0	17%
fuselage group	483.6	554.5	15%
alighting gear	291.4	332.2	14%
engine section/nacelle	189.5	100.7	-47%
PROPULSION GROUP (including fuel)	1449.5	2270.8	57%
engine system	844.6	438.3	-48%
fuel system (+fuel)	312.7	1608.8	414%
drive system	292.2	223.7	-23%
SYSTEM AND EQUIP	951.3	1042.2	10%
flight controls	404.1	467.4	16%
hydraulic group	126.3	149.3	18%
electric group	84.6	87.8	4%

C. **Performance**

Table 7 compares the sizing mission performance and off-design performance of turboelectric and full-electric designs. Although the turboelectric variant is lighter due to the high energy density of jet-A fuel, it consumes significantly more energy because the turboshaft engine has a higher energy demand compared to the battery in the full-electric design. The turboelectric design outpaced the full-electric in both mission and off-design speeds. The turboelectric variant achieved a mission block speed of approximately 15 knots higher, a best range speed of about 25 knots higher, and a maximum speed of 10 knots higher than the full-electric design.

Fig. 7 shows the total power required and power available during the mission. For both full-electric and turboelectric variants, all engine group components (electric motors, turboshaft engine, and generator) were sized at the first vertical takeoff segment. In the second takeoff segment, the power requirement remained the same for the full-electric design but decreased for the turboelectric variant as fuel was consumed. The power values for the turboelectric variant were higher than those for the full-electric design because, in addition to the electric motors, the turboshaft and generator power had to be included.

According to [7], the segments that sized propulsion systems of tiltrotor reference vehicles differed between turboshaft and electric versions. The vehicle was sized at the first vertical takeoff segment for the turboshaft version, similar to the turboelectric six-tiltrotor shown in Fig. 7. In contrast, the electric version was sized at the climb segment, providing an additional power margin in helicopter modes. This meant that the motors were sized heavier than they would have been if the vehicle had been sized at the takeoff segment. Consequently, the design gross weight increased by 64% from the turboshaft to the electric tiltrotor reference vehicle. Conversely, in the case of the six-tiltrotor, it can be inferred that the ratio of weight increase from the turboelectric to full-electric was less significant (22%) because both vehicles were sized at the same mission segment.

Table 7 Sizing mission and off-design performance

Sizing Mission Performance	Turboelectric (lb)	Full-Electric (lb)
Fuel Burn (lb)	141.1	-
Energy Burn (MJ)	2738.6	784.4
Air Distance (nm)	79.8	80.8
Block Time (min.)	33.6	38.6
Block Speed (kts)	133.8	116.7
Fuel Flow (lb/hr)	254.1	-
Energy Flow (MJ/hr)	4932.4	1220.5
Specific Range (nm/lb)	0.527	-
Specific Range (nm/MJ)	0.027	0.096
Energy Efficiency (ton-nm/lb)	0.316	-
Energy Efficiency (ton-nm/MJ)	0.016	0.057
Yearly Operating Cost ($)	3,921,843	2,578,098
Cost Per Trip ($)	795	579
Off-design Mission Performance		
V_{br} at DGW 6K ISA (kts)	154.3	129.3
V_{max} at DGW 6K ISA (kts)	203.5	193.3

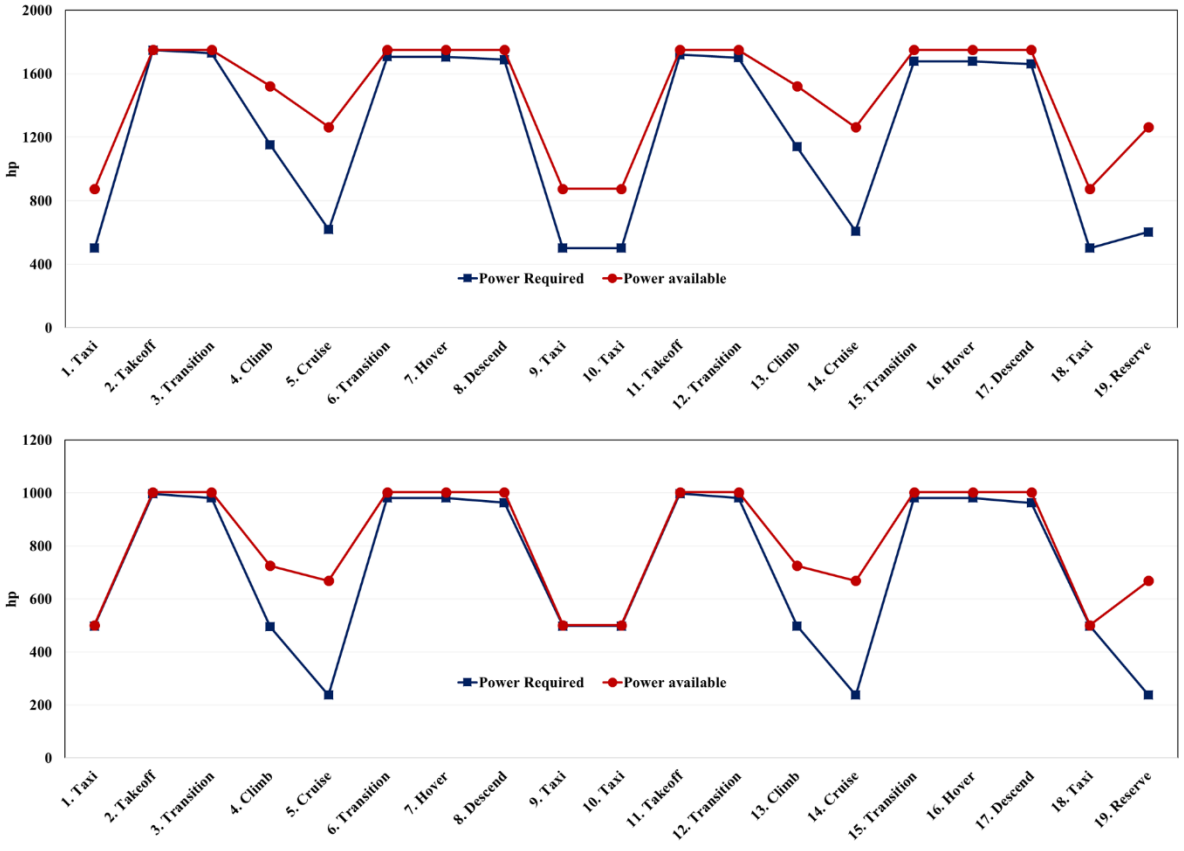

Fig. 7 Mission power for turboelectric (top) and full-electric (bottom)

D. Comparison with other reference vehicles

Table 8 compares the six-tiltrotor designs with other six-passenger NASA UAM reference vehicles. Each design's NDARC model, sourced from [15], was individually executed. Therefore, some differences may exist compared to other papers due to ongoing updates to the models and NDARC code. In the table, TS refers to turboshaft, E to electric, and TE to turboelectric. The reference vehicles for comparison were selected based on their propulsion systems and configuration similarities, with the quadrotor serving as the baseline for edgewise-flying UAM.

Table 8 Comparison of the six-tiltrotor vehicle with other six-passenger NASA UAM reference vehicles

Vehicle	Quad TS	Quad E	L+C TE	L+C E	Tiltwing TE	TR TS	TR E	6TR TE	6TR E
Lifter disk loading (psf)	3.5	3.0	10.6	15.0	20.0	12.0	10.0	16.0	16.0
Lifter radius	9.20	13.06	5.00	5.00	3.66	7.55	10.95	4.25	4.69
Solidity, thrust-weighted	0.065	0.056	0.177	0.249	0.247	0.171	0.143	0.228	0.228
Number of lift engine/motor	1	4	8	8	8	2	2	6	6
MRP power per lifter (hp)	305	167	114	187	227	411	682	138	167
Cruise drag *D/q* (ft2)	7.19	12.85	11.67	13.65	7.05	3.93	4.63	4.58	4.75
Battery system weight (lb)	-	2015	299	2650	567	-	2060	48	1608
Energy burn (MJ)	2658	1058	3781	1355	3280	2738	1015	2739	784
Block time (min)	42.8	51.5	42.9	45.3	38.0	32.3	31.4	33.6	38.6
Block speed (kt)	105.2	87.3	104.8	99.3	118.5	139.1	143.3	133.8	116.7
Design gross weight (lb)	3723	6427	6678	9408	6713	4300	7530	5450	6636
Vbr at DGW 6kISA (kt)	122	98	94	95	148	170	165	154	129
Vmax at DGW 6kISA (kt)	142	110	138	138	194	204	223	204	194
Trip Operating Cost ($)	611	836	1177	1191	1294	473	544	795	579

The six-tiltrotor reference vehicles featured higher rotor disk loading than most existing reference vehicles, except for the tiltwing, resulting in a smaller rotor radius. They exhibited the lowest energy consumption among designs with the same propulsion systems, which was reflected in their weight. Among turboelectric reference vehicles, the turboelectric six-tiltrotor was the fastest available. Although the electric six-tiltrotor was slower than the electric tiltrotor, its multiple rotor design enhances safety, making it a competitive choice where safety is a priority.

VI. Conclusion

Full-electric and turboelectric six-tiltrotor reference vehicles were newly designed as part of NASA's UAM reference vehicle suite. Building on the existing tiltrotor reference vehicle, several unique design considerations for the six-tiltrotor were implemented into the NDARC model. While RPM-controlled designs were considered, collective-controlled designs were ultimately selected for the initial six-tiltrotor models. The full-electric variant was heavier, had a larger footprint, and was slower than the turboelectric variant. However, the full-electric design is preferable when environmental impact is a priority. Compared to other reference vehicles, the six-tiltrotor models were competitive, featuring lower energy consumption, reduced weight, increased redundancy, and respectable speed. Further studies are recommended to develop a dedicated rotor performance model for the six-tiltrotor, explore the design space of RPM-controlled variants, and develop a multirotor wing model.

Appendix

Figure A1: Six-tiltrotor Hover Mode

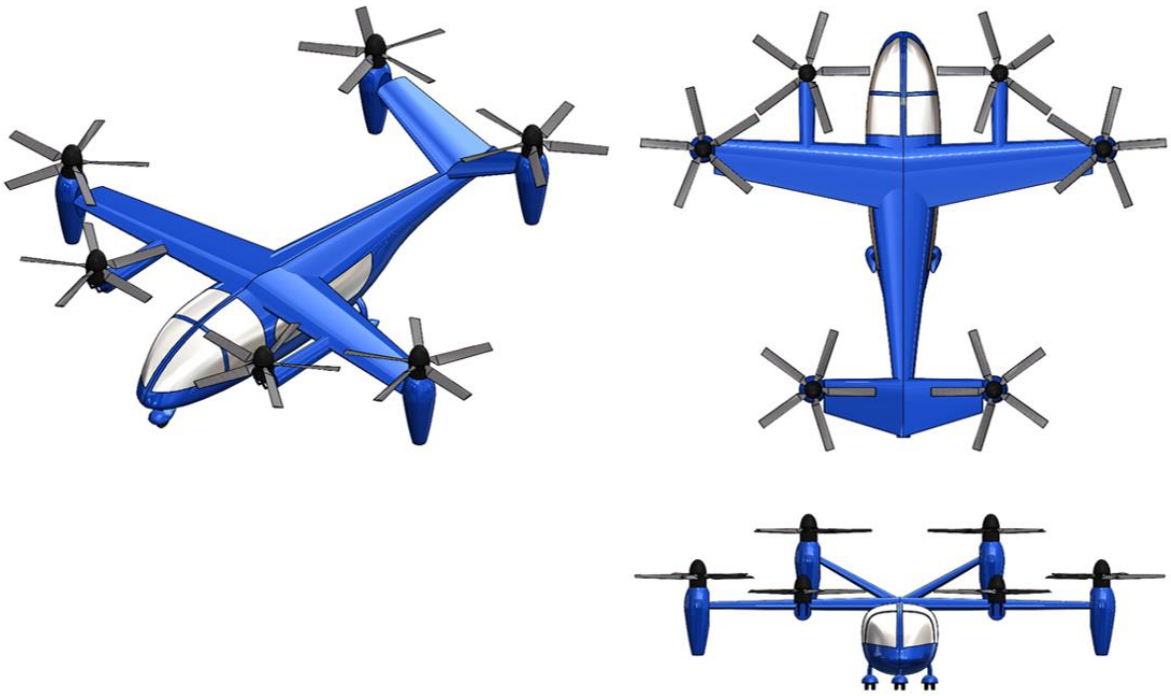

Figure A2: Six-tiltrotor Cruise Mode

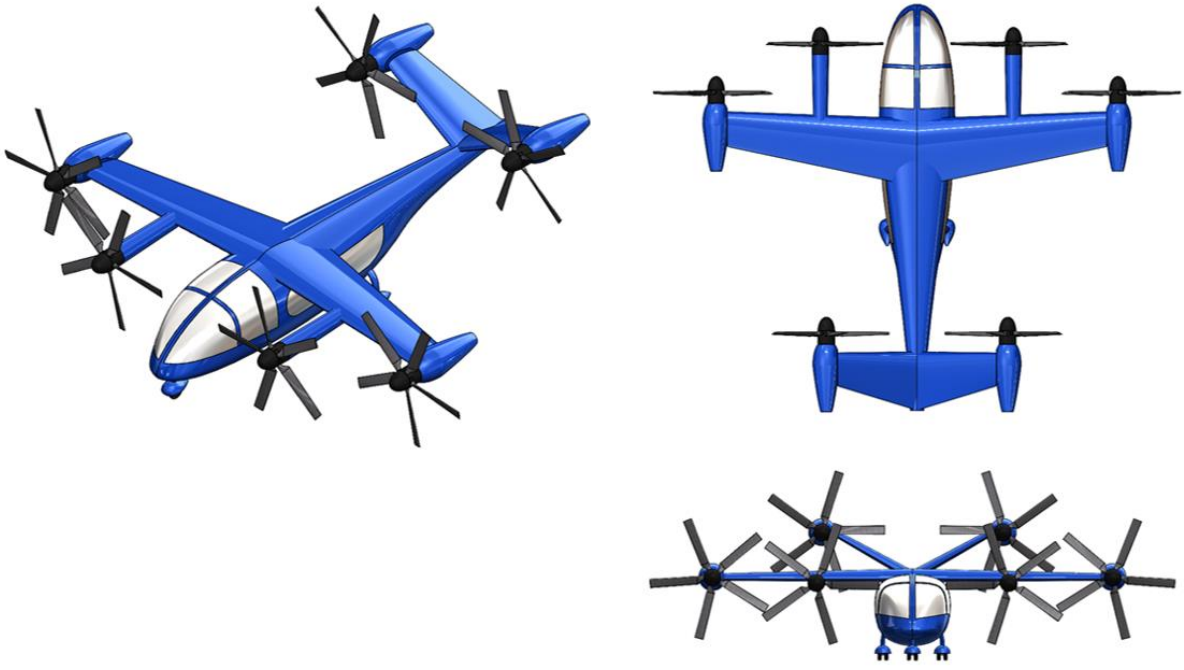

Acknowledgments

This work is the outcome of an international internship program at NASA Ames Research Center. The first author would like to thank Michael Radotich, Dr. Wayne Johnson, and Christopher Silva for their invaluable assistance and direction during an internship in the Aeromechanics branch. Furthermore, the first author deeply appreciates Dr. William Warmbrodt for his support and the profound insights he provided.

References

[1] The Vertical Flight Society eVTOL Aircraft Directory, Accessed 06/21/2024. https://evtol.news/aircraft

[2] Johnson, W., Silva, C., and Solis, E., "Concept vehicles for VTOL air taxi operations.", *AHS Specialists Conference on Aeromechanics Design for Transformative Vertical Flight*, San Fransisco, CA, 2018.

[3] Silva, C., Johnson, W., Solis, E., Patterson, D., and Antcliff, R. "VTOL urban air mobility concept vehicles for technology development.", *2018 Aviation Technology, Integration, and Operations Conference*, Atlanta, GA, 2018.

[4] Johnson, W., "A quiet helicopter for air taxi operations," *Aeromechanics for Advanced Vertical Flight Technical Meeting*, San Jose, CA, 2020.

[5] Whiteside, S. K., and Pollard, B. P. "Conceptual Design of a Tiltduct Reference Vehicle for Urban Air Mobility," *Aeromechanics for Advanced Vertical Flight Technical Meeting, Transformative Vertical Flight 2022*, San Jose, CA, 2022

[6] Whiteside, S. K., Pollard, B. P., Antcliff, K. R., Zawodny, N. S., Fei, X., Silva, C., and Medina, G. L. "Design of a Tiltwing Concept Vehicle for Urban Air Mobility," *NASA/TM-20210017971*, NASA, Hampton, VA, 2021.

[7] Radotich, M., "Conceptual Design of Tiltrotor Aircraft for Urban Air Mobility," *VFS Aeromechanics for Advanced Vertical Flight Technical Meeting*, San Jose, CA, 2022.

[8] Pollard, B. P., Welstead, J. R., and Whiteside, S. K., "Design of a Multi-Tiltrotor Concept Vehicle for Urban Air Mobility:"Version 0" Design, Design Review: Nov 3, 2021," *retrieved from https://sacd.larc.nasa.gov/wp-content/uploads/sites/167/2023/07/202305-Multi-Tiltrotor-Publication.pdf*, Hampton, VA, 2021.

[9] Cornelius, J. K., "Designing a Coaxial Quadrotor for Urban Air Mobility," *10th Biennial Autonomous VTOL Technical Meeting & 10th Annual Electric VTOL Symposium*, Mesa, AZ, 2023.

[10] Johnson, W., "NDARC NASA Design and Analysis of Rotorcraft," *NASA/TP-2015-218751*, NASA, Moffett Field, CA, 2015

[11] Silva, C., Johnson, W., and Solis, E., "Multidisciplinary conceptual design for reduced-emission rotorcraft," *AHS Specialists Conference on Aeromechanics Design for Transformative Vertical Flight*, San Fransisco, CA, 2018.

[12] Johnson, W., *CAMRAD-II Theory*, Johnson Aeronautics, 2022.

[13] Patterson, M. D., Antcliff, K. R., and Kohlman, L., W., "A proposed approach to studying urban air mobility missions including an initial exploration of mission requirements," *AHS International 74th Annual Forum & Technology Display*, Phoenix, AZ, 2024.

[14] Malpica, C., Suh, P., and Silva, C., "Flight Dynamics Conceptual Design Exploration of Multirotor eVTOL," *80th Vertical Flight Society's (VFS) Annual Forum & Technology Display*, Montreal, Canada, 2024.

[15] NASA Urban Air Mobility (UAM) Reference Vehicles, Systems Analysis and Concepts Directorate, NASA, Accessed 06/21/2024. https://sacd.larc.nasa.gov/uam-refs/